

p–*T*–*x* Measurements for Some Working Fluids for an Absorption Heat Transformer: 1,1,1,2-Tetrafluoroethane (R134a) + Dimethylether Diethylene Glycol (DMEDEG) and Dimethylether Triethylene Glycol (DMETrEG)

Raouf Zehioua,^{†,‡} Christophe Coquelet,[‡] Abdeslam-Hassen Meniai,[†] and Dominique Richon^{*,‡}

Laboratoire de l'Ingénierie des Procédés de l'Environnement (LIPE), Département de Chimie Industrielle, Université Mentouri Constantine, Route Ain El Bey, Constantine 25017, Algérie, and Mines ParisTech, CEP/TEP-Centre Energétique et Procédés, 35 Rue Saint Honoré, 77305 Fontainebleau, France

The solubilities of 1,1,1,2-tetrafluoroethane (R134a), $\text{CF}_3\text{CH}_2\text{F}$, + dimethylether diethylene glycol (DMEDEG), $\text{CH}_3\text{O}(\text{CH}_2\text{CH}_2\text{O})_2\text{CH}_3$, and R134a + dimethylether triethylene glycol (DMETrEG) binary systems were measured, using the “static–analytic” method at temperatures between (303 and 353) K. This work was an opportunity to test the use of R134a as a refrigerant in combination with an organic absorbent, like DMEDEG and DMETrEG, in an absorption heat transformer (AHT), also known as a type II absorption heat pump or a reversed absorption heat pump. The experimental data were correlated using the Peng–Robinson equation of state (PR-EoS) in combination with Mathias–Copeman α function, Huron–Vidal mixing rules, and the nonrandom two-liquid (NRTL) activity coefficient model. The experimental results were compared to the predicted values obtained using the predictive Soave–Redlich–Kwong group contribution equation of state (PSRK-EoS).

1. Introduction

The damages that may be caused to the ozone layer by chlorofluorocarbons (CFC's) and hydrochlorofluorocarbons (HCFC's) have encouraged not only the development of alternative compounds but also that of new machines such as those based on absorption cycles where the available waste heat can be favorably used. Consequently, this has stimulated the investigation and test of new working fluids, upon which the machine performance depends. Therefore, it is necessary to know the influence of most thermodynamic properties of the involved pure components on the performance of absorption cycles.

In fact, absorption heat transformers (AHTs) are a particular type of absorption heat pump where waste heat can be upgraded without the need of an external heat source. Basically, a single stage AHT (see Figure 1) consists of a generator (GE), an absorber (AB), an evaporator (EV), a condenser (CO), a heat exchanger (HEX), pumps, and throttle.¹

The present work considers the analysis of the behavior of an AHT, operating with the above cited working pairs at the following assumed temperature ranges for the different cycle parts: $283 \leq T_{\text{CO}} \leq 313$ K, $323 \leq T_{\text{GE}} (T_{\text{EV}}) \leq 343$ K, and $353 \leq T_{\text{AB}} \leq 393$ K.

Ammonia/water and water/lithium bromide mixtures are conventional absorption working fluids.³ An H_2O –LiBr working fluid is used in commercial AHTs; the advantages of this working fluid are a high enthalpy of evaporation and good thermodynamic properties, such as being nontoxic, nonexplosive, nonflammable, and so forth. An NH_3 – H_2O working fluid is used in absorption refrigeration systems,

because of its interesting thermodynamic properties.⁴ However, despite their advantages, these working fluids have some drawbacks. Ammonia is volatile, toxic, and flammable and is corrosive toward copper. When used as a working fluid in heat transformers its application range is limited because of its high working pressure and its poor safety level. Similarly, the use of H_2O –LiBr solution at high temperatures or concentrations is limited by corrosion or crystallization.^{5,6}

To estimate the performance of the refrigerant–absorbent candidate pairs in a refrigeration or heat pump cycle in terms of the coefficient of performance (COP) and the circulation ratio (defined as the ratio of the mass flow rate of the strong solution to the mass flow rate of the refrigerant), the thermophysical properties of the pure components and of the mixtures, the equilibrium and transport properties, and the thermal stability of the refrigerant–absorbent pairs have to be determined.⁷

In the literature, a great number of research studies were concerned with the screening of the best “refrigerant–absorbent” pairs, according to specific applications and properties. The most desirable ones in absorption working fluids³ are summarized in Table 1. For instance, one can cite Fatouh and Murthy⁸ who made a comparative study of different working fluids, using R22 as refrigerant and six organic absorbents [*N,N*-dimethylformamide (DMF), *N,N*-dimethylacetamide (DMA), *N*-methyl-2-pyrrolidone (NMP), dimethylether diethylene glycol (DMEDEG), dimethylether tetraethylene glycol (DMETEG), and dimethylether triethylene glycol (DMETrEG)] in a vapor AHT, on the basis of *p*–*T*–*x*–*H* data. Similarly Borde et al.⁹ considered the use of the refrigerant 1,1,1,2-tetrafluoroethane (R134a) as a substitute to CFC's in absorption heat pumps and refrigeration units and tested it in combination with different commercial absorbents such as dimethylether tetraethylene glycol (DME-TEG), *N*-methyl ϵ -caprolactam (MCL), or dimethylethyleneurea (DMEU), in absorption systems. Interesting results

* Corresponding author. E-mail: dominique.richon@mines-paristech.fr.

[†] Université Mentouri Constantine.

[‡] Mines ParisTech, CEP/TEP-Centre Energétique et Procédés.

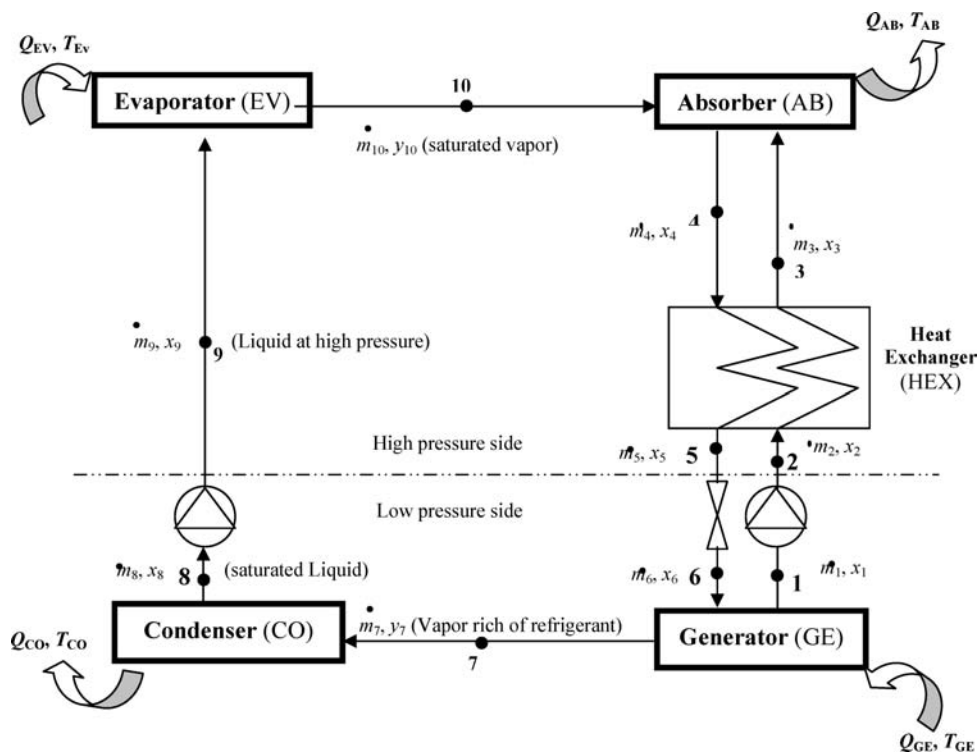


Figure 1. Single stage of an absorption heat transformer (AHT).

Table 1. Absorption Working Fluids Properties³

fluid	required property	observed property	
		ammonia/water	water/lithium bromide
refrigerant	high latent heat	good	excellent
	moderate vapor pressure	too high	too low
	low freezing temperature	excellent	limited application
absorbent	low viscosity	good	good
	low vapor pressure	poor	excellent
mixture	low viscosity	good	good
	no solid phase	excellent	limited application
	low toxicity	poor	good
	high affinity between refrigerant and absorbent	good	good

Table 2. Suppliers and Mass Fraction w Purities of the Used Chemicals

chemical	supplier	w
R134a	Arkema	0.995
DMEDEG	Acros	0.99
DMETrEG	Aldrich	0.99

were obtained indicating that the R134a–DMETEG pair was the most performing.⁹ This has stimulated and encouraged the test of this refrigerant with further organic absorbents such as the DMEDEG and DMETrEG in an AHT.

From a careful literature search, some publications have been found such as vapor–liquid equilibrium (VLE) data concerning the R134a–DMETrEG pair by Coronas et al.¹⁰ using the static method at temperatures between (283.15 and 353.15) K. Marchi et al.¹¹ measured the bubble pressures of the R134a–DMETrEG system at temperatures between (283 and 323) K using a computer-operated static apparatus, mainly for R134a liquid molar fraction higher than 0.7. López et al.¹² presented experimental solubilities of R134a in

Table 3. Critical Parameters²²

chemical	p_c /MPa	T_c /K	CAS Registry No.
R134a	4.064	374.25	811-97-2
DMEDEG	2.860	608.00	111-96-6
DMETrEG	2.310	651.00	112-49-2

Table 4. Experimental and Calculated R134a Vapor Pressures (Using the PR-EoS with the Mathias–Copeman α Function)

T	p_{exp}	p_{cal}	Δp
K	MPa	MPa	MPa
303.45	0.7757	0.7755	0.0002
308.44	0.8922	0.8927	-0.0005
313.30	1.0188	1.0188	0.0000
318.39	1.1654	1.1648	0.0006
323.30	1.3190	1.3198	-0.0008
328.26	1.4924	1.4918	0.0006
333.30	1.6837	1.6835	0.0002
338.24	1.8896	1.8891	0.0005
343.23	2.1153	2.1161	-0.0008

DMETrEG and DMEDEG at 101.33 kPa between (258.15 and 298.15) K. Furthermore, for R134a + DMETrEG system, additional measurements of densities^{13,14} and viscosities¹⁵ were carried out. No VLE data were found in literature for the R134a + DMEDEG system.

Herein, we present new p – T – x data for R134a + DMEDEG and DMETrEG systems that have been measured and correlated as shown in the following section. The International Union of Pure and Applied Chemistry (IUPAC) systematic name for DMEDEG is 1-methoxy-2-(2-methoxyethoxy)ethane, while for DMETrEG it is 1,2-bis(2-methoxyethoxy)ethane.

2. Experimental Section

2.1. Materials. The sources and the purities of the used chemicals, as certified by the manufacturers, are presented in Table 2. No further purification or pretreatment were performed except for the careful degassing of DMEDEG and DMETrEG. Degassing was obtained under vacuum provided

Table 5. Mathias–Copeman Parameters

coefficients	R134a ^a	R134a ^b	DMEDEG ^c	DMEDEG ^d	DMETrEG ^e	DMETrEG ^f
c_1	1.105	0.919	1.256	1.461	1.488	1.714
c_2	-1.856	-1.281	-0.614	-1.084	-0.238	-0.767
c_3	7.385	5.958	1.123	1.750	0.474	1.215

^a Mathias–Copeman parameters adjusted for the PR-EoS. ^b Mathias–Copeman parameters adjusted for the Soave–Redlich–Kwong equation of state (SRK EoS). ^c Mathias–Copeman parameters for the PR EoS.²⁴ ^d Mathias–Copeman parameters for the SRK EoS.²⁴ ^e Mathias–Copeman parameters for the PR EoS.²⁴ ^f Mathias–Copeman parameters for the SRK EoS.²⁴

by a vacuum pump (Trivac E2 from Oerlikon, Germany) for about 1 h of the heated ($T = 373$ K) and efficiently stirred chemicals.

2.2. Apparatus and Experimental Procedure. The measurements of p – T – x data of R134a + DMEDEG, DMETrEG binary systems were made using a “static–analytic” tech-

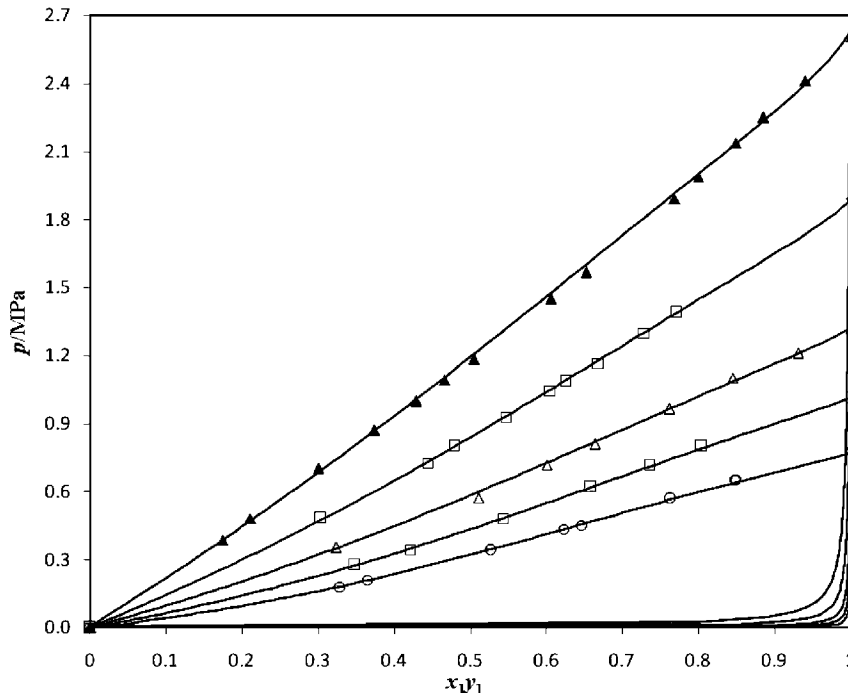


Figure 2. VLE isotherms for the R134a (1) + DMEDEG (2) binary system; ○, 303 K; □, 313 K; △, 323 K; ◇, 338 K; ▲, 353 K. Solid lines are calculated results using our model.

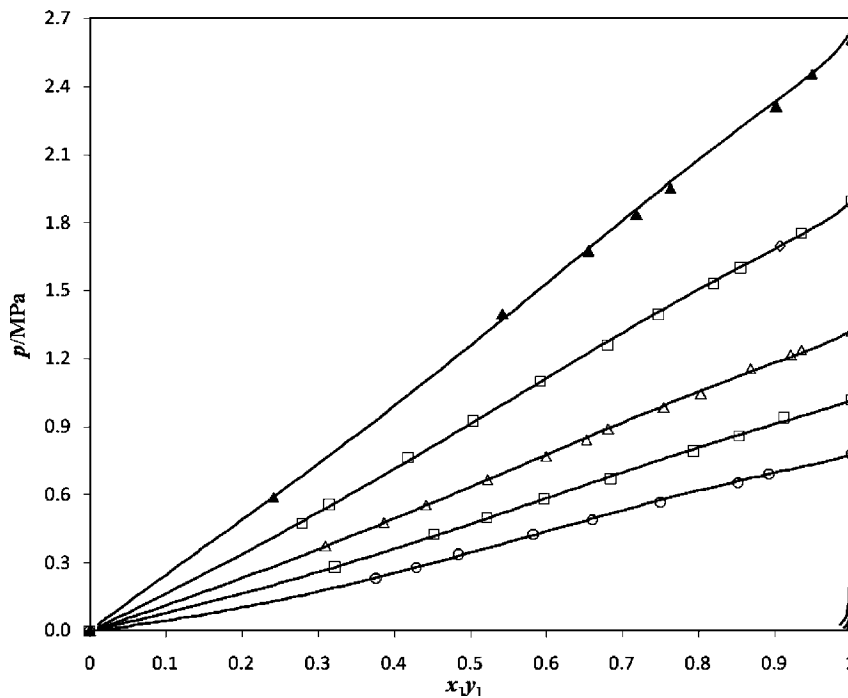


Figure 3. Vapor–liquid equilibrium isotherms for the R134a (1) + DMETrEG (2) binary system; ○, 303 K; □, 313 K; △, 323 K; ◇, 338 K; ▲, 353 K. Solid lines are calculated results using our model.

nique. This latter was already reported in details by Laugier and Richon.¹⁶ The description of the used apparatus and its corresponding experimental procedure was given by Zehioua et al.¹⁷ The equilibrium temperature was measured using two Pt-100 platinum probes. A 25 Ω reference platinum probe (Tinsley, France) was used to calibrate both temperature sensors; the uncertainty in the temperature measurements was estimated to be within ± 0.02 K. The equilibrium pressure is measured using a Druck pressure transducer (up to 4.0 MPa) which is calibrated by means of a dead weight balance (Desgranges and Huot model 5202S, France). The estimated uncertainty on pressure measurements is within ± 1 kPa.

Liquid samples were analyzed by means of a gas chromatograph (Varian, CP-3800), using a thermal conductivity detector (TCD). The calibration of the TCD was made by introducing a known pure component volumes with appropriate syringes. The uncertainty on liquid mole fractions was estimated to be ± 3 %. The chromatographic column used is RTX-5-amine (3 μ m, 15 m \times 0.53 mm i.d.) from Restek, France.

3. Correlation

The correlation of the VLE experimental measurements is obtained by the combination of Peng–Robinson¹⁸ equation of state (PR-EoS) with the Mathias–Copeman¹⁹ α function, Huron–Vidal²⁰ mixing rules, and the nonrandom two-liquid (NRTL)²¹ activity coefficient model.

The critical properties²² of the considered components are indicated in Table 3.

The Mathias–Copeman α function¹⁹ for $T < T_C$ is expressed as follows

$$\alpha(T) = \left[1 + c_1 \left(1 - \sqrt{\frac{T}{T_C}} \right) + c_2 \left(1 - \sqrt{\frac{T}{T_C}} \right)^2 + c_3 \left(1 - \sqrt{\frac{T}{T_C}} \right)^3 \right]^2 \quad (1)$$

where c_1 , c_2 , and c_3 are adjustable parameters.

The Huron–Vidal mixing rule²⁰ is presented as:

$$a = b \left(\sum_i x_i \left(\frac{a_i}{b_i} \right) + g_{P=\infty}^E \cdot C \right) \quad (2)$$

$$b = \sum_i x_i b_i \quad (3)$$

where a_i and b_i are respectively the attractive parameter and the molar covolume.

The excess Gibbs energy model based on the NRTL activity coefficient model²¹ is given by:

$$\frac{g^E(T, p, x_i)}{RT} = -q \sum_{i=1}^n x_i \ln \left(\sum_{j=1}^n G_{ji} x_j \right) + p \sum_{i=1}^n x_i \frac{\sum_{j=1}^n \tau_{ji} G_{ji} x_j}{\sum_{k=1}^n G_{ki} \tau_k} \quad (4)$$

where n is the number of components in the system and

$$G_{ji} = \exp(-\alpha_{ji} \tau_{ji}) \quad (5)$$

$$\tau_{ji} = \frac{(g_{ji} - g_{ii})}{RT} \quad (6)$$

$\tau_{ii} = 0$ and $\alpha_{ii} = 0$.

Table 6. Experimental and Calculated VLE Data for the R134a + DMEDEG and R134a + DMETrEG Binary Mixtures at Different Temperatures

	P_{exp}	P_{cal}	$x_{1,\text{exp}}$	$(y_{2,\text{cal}}) \cdot 10^2$	$\Delta p/p_{\text{exp}}$	
	MPa	MPa			%	
R134a (1) + DMEDEG (2)						
$T = 303.30$ K	0.1817	0.1828	0.329	0.122	-0.62	
	0.2119	0.2092	0.364	0.101	1.28	
	0.3416	0.3454	0.526	0.047	-1.10	
	0.4350	0.4343	0.623	0.031	0.17	
	0.4526	0.4561	0.646	0.028	-0.78	
	0.5687	0.5658	0.763	0.016	0.51	
	0.6524	0.6407	0.847	0.009	1.79	
$T = 313.20$ K	0.6544	0.6422	0.849	0.009	1.87	
	0.2777	0.2749	0.348	0.163	1.03	
	0.3445	0.3487	0.421	0.118	-1.21	
	0.4808	0.4837	0.543	0.072	-0.61	
	0.6203	0.6186	0.658	0.045	0.27	
	0.7155	0.7111	0.736	0.032	0.62	
	0.8013	0.7915	0.804	0.023	1.22	
$T = 323.30$ K	0.3544	0.3508	0.323	0.260	1.02	
	0.5718	0.5826	0.511	0.129	-1.89	
	0.7183	0.7285	0.601	0.095	-1.42	
	0.8106	0.8210	0.664	0.076	-1.29	
	0.9641	0.9649	0.762	0.052	-0.08	
	1.1005	1.0848	0.845	0.035	1.43	
	1.2093	1.2093	0.931	0.018	0.00	
$T = 338.15$ K	0.4830	0.4752	0.303	0.476	1.61	
	0.7257	0.7326	0.444	0.290	-0.94	
	0.8013	0.7995	0.479	0.260	0.23	
	0.9293	0.9321	0.546	0.213	-0.31	
	1.0450	1.0504	0.605	0.180	-0.52	
	1.0845	1.0906	0.625	0.170	-0.56	
	1.1642	1.1792	0.668	0.150	-1.29	
$T = 353.15$ K	1.2973	1.3022	0.729	0.124	-0.38	
	1.3905	1.3878	0.771	0.108	0.19	
	0.3859	0.3874	0.174	1.343	-0.40	
	0.4810	0.4716	0.211	1.106	1.94	
	0.7021	0.6852	0.300	0.764	2.40	
	0.8699	0.8687	0.374	0.603	0.14	
	0.9995	1.0098	0.429	0.517	-1.03	
R134a (1) + DMETrEG (2)	1.0913	1.1055	0.466	0.471	-1.30	
	1.1848	1.2070	0.505	0.429	-1.87	
	1.4512	1.4778	0.606	0.342	-1.83	
	1.5673	1.6016	0.652	0.310	-2.19	
	1.8916	1.9162	0.768	0.237	-1.30	
	1.9868	2.0008	0.800	0.218	-0.70	
	2.1374	2.1336	0.849	0.187	0.18	
	2.2501	2.2353	0.885	0.161	0.66	
	2.4113	2.3990	0.941	0.110	0.51	
	$T = 303.45$ K	0.2322	0.2342	0.376	0.003	-0.87
		0.2805	0.2795	0.429	0.002	0.35
0.3327		0.3291	0.484	0.002	1.06	
0.4246		0.4219	0.583	0.001	0.63	
0.4911		0.4939	0.660	0.001	-0.57	
0.5673		0.5760	0.750	0.001	-1.52	
0.6545		0.6597	0.851	0.001	-0.79	
$T = 313.24$ K	0.6920	0.6915	0.893	0.001	0.08	
	0.2775	0.2811	0.323	0.006	-1.28	
	0.4249	0.4164	0.452	0.004	2.00	
	0.4995	0.4940	0.521	0.003	1.11	
	0.5789	0.5802	0.597	0.002	-0.22	
	0.6696	0.6813	0.685	0.002	-1.74	
	0.7895	0.8022	0.794	0.001	-1.61	
$T = 323.33$ K	0.8601	0.8635	0.853	0.001	-0.39	
	0.9341	0.9223	0.912	0.001	1.27	
	0.3736	0.3729	0.310	0.012	0.21	
	0.4783	0.4758	0.387	0.009	0.53	
	0.5533	0.5513	0.441	0.008	0.37	
	0.6660	0.6660	0.522	0.006	-0.01	
	0.7702	0.7765	0.600	0.005	-0.81	
$T = 338.30$ K	0.8430	0.8514	0.652	0.004	-0.99	
	0.8896	0.8918	0.681	0.004	-0.25	
	0.9851	0.9932	0.754	0.003	-0.82	
	1.0452	1.0584	0.803	0.003	-1.26	
	1.1556	1.1417	0.868	0.002	1.20	
	1.2158	1.2076	0.921	0.001	0.67	
	1.2368	1.2250	0.935	0.001	0.95	
	0.473	0.481	0.279	0.030	-1.70	
	0.552	0.549	0.315	0.027	0.52	
	0.766	0.750	0.419	0.020	2.03	
	0.923	0.917	0.503	0.017	0.59	
$T = 353.33$ K	1.099	1.097	0.592	0.014	0.22	
	1.260	1.277	0.681	0.011	-1.30	
	1.390	1.407	0.748	0.010	-1.25	
	1.528	1.541	0.819	0.008	-0.86	
	1.596	1.606	0.856	0.007	-0.60	
	1.695	1.695	0.906	0.006	0.00	
	1.753	1.746	0.935	0.005	0.43	
	0.588	0.590	0.241	0.074	-0.24	
	1.397	1.374	0.543	0.038	1.63	
	1.673	1.683	0.654	0.033	-0.58	
	1.835	1.858	0.718	0.031	-1.25	
1.951	1.980	0.763	0.029	-1.50		
2.310	2.337	0.902	0.022	-1.19		
2.453	2.458	0.949	0.017	-0.19		

$\alpha_{ij} = \alpha_{ji}$, τ_{ij} , and τ_{ji} are adjustable parameters. α_{ij} is the nonrandomness parameter, taken equal to 0.3 in this work. The Simplex algorithm²³ was used to minimize the following objective function:

$$F = \frac{100}{N} \left[\sum_1^N \left(\frac{p_{i,\text{exp}} - p_{i,\text{cal}}}{p_{i,\text{exp}}} \right)^2 \right] \quad (7)$$

where N is the number of experimental data and p_{exp} and p_{cal} are respectively the experimental and the calculated pressures.

4. Results and Discussion

To analyze and evaluate the performance of the model used to correlate the experimental data, the following relative deviations of p , the average absolute deviation (AADP) and the measurement bias (BIASP), are calculated as:

$$\text{AADP} = (100/N) \sum_{i=1}^N \left| \frac{(p_{i,\text{exp}} - p_{i,\text{cal}})}{p_{i,\text{exp}}} \right| \quad (8)$$

$$\text{BIASP} = (100/N) \sum_{i=1}^N \left(\frac{(p_{i,\text{exp}} - p_{i,\text{cal}})}{p_{i,\text{exp}}} \right) \quad (9)$$

where N is the number of experimental measurements.

4.1. Pure Component Vapor Pressure. The vapor pressure of R134a was measured at temperatures between (298 and 353) K, well-correlated using our previously defined model, and used to adjust Mathias–Copeman parameters. The experimental results are shown in Table 4. The Mathias–Copeman parameters²⁴ of DMEDEG and DMETrEG are reported in Table 5 along with our R134a Mathias–Copeman adjusted parameters.

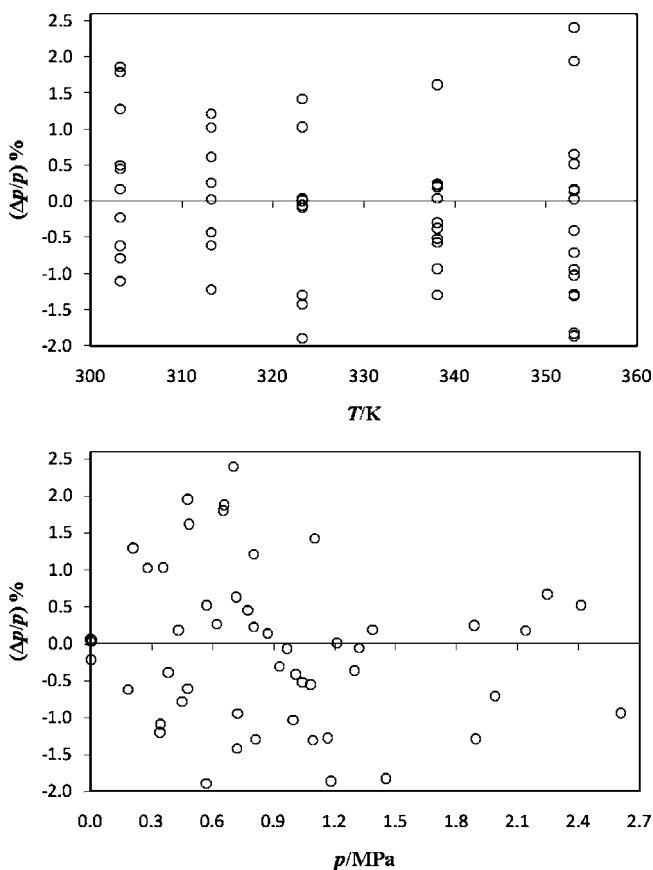


Figure 4. Relative pressure deviations between the measured and the calculated data using our model, for the R134a (1) + DMEDEG (2) system.

Table 7. NRTL Adjusted Parameters for Huron–Vidal Mixing Rules

R134a (1) + DMEDEG (2)			R134a (1) + DMETrEG (2)		
T	τ_{12}	τ_{21}	T	τ_{12}	τ_{21}
K	$\text{J}\cdot\text{mol}^{-1}$	$\text{J}\cdot\text{mol}^{-1}$	K	$\text{J}\cdot\text{mol}^{-1}$	$\text{J}\cdot\text{mol}^{-1}$
303.30	-460	-1498	303.45	-1396	-339
313.20	805	-2139	313.24	1180	-1920
323.30	2427	-2782	323.33	1776	-1953
338.15	2187	-2458	338.30	1616	-1695
353.15	1440	-1551	353.33	-1902	2552

For DMEDEG and DMETrEG, no new vapor pressure measurements have been carried out.

4.2. VLE for the R134a + DMEDEG and R134a + DMETrEG Binary Mixtures. The experimental and calculated isothermal VLE data for the R134a + DMEDEG and R134a + DMETrEG binary systems at different temperatures are presented in Table 6 and plotted in Figures 2 and 3.

The NRTL parameters for Huron–Vidal mixing rules that were adjusted on our data, at each temperature, are listed in Table 7. A good representation of data (small values of deviation) is obtained as displayed in Figure 4. The experimental data of Coronas et al.¹⁰ and Marchi et al.¹¹ are compared to the results obtained from the proposed model; corresponding deviations in pressure are plotted in Figure 5. The BIASP and AADP values are listed in Table 8.

Figure 5 shows that the experimental data of Coronas et al.¹⁰ deviate significantly from data calculated using the present model and adjusted NRTL parameters, which is not the case of those from Marchi et al.¹¹

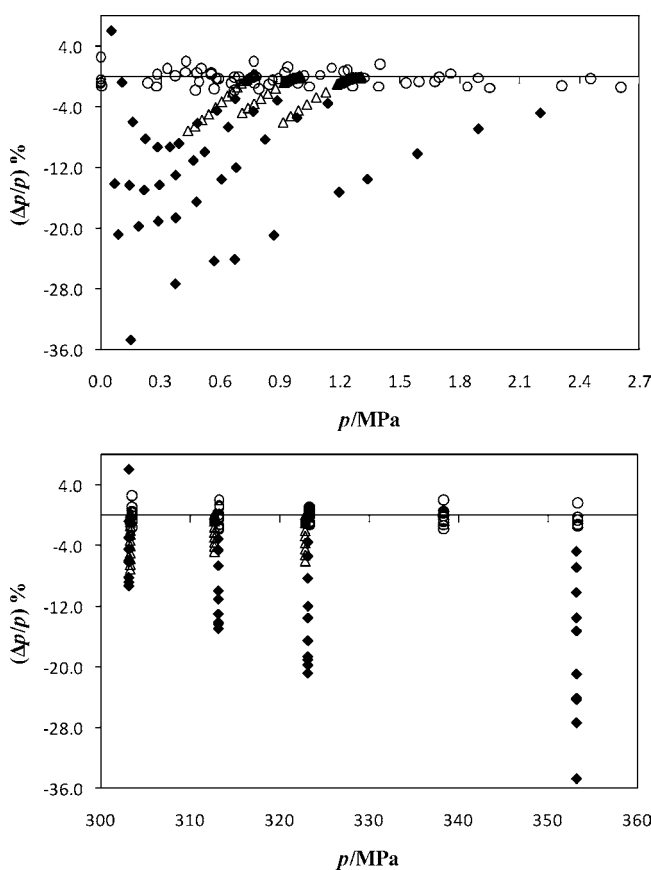


Figure 5. Relative pressure deviations between experimental and calculated data using our model, for the R134a (1) + DMETrEG (2) system: \circ , this work; \blacklozenge , Coronas et al.;¹⁰ \triangle , Marchi et al.¹¹

Table 8. Relative Deviations BIASP and AADP Using PR-EoS with the Huron–Vidal Mixing Rules, Mathias–Copeman α Function, and NRTL Activity Coefficient Model

R134a(1) + DMEDEG (2)				
T		N^a	BIASP	AADP
K			%	%
303.30		10	0.34	0.88
313.20		8	0.12	0.68
323.30		9	-0.25	0.80
338.15		11	-0.15	0.57
353.15		16	-0.36	1.09

R134a(1) + DMETrEG (2)											
present work				Coronas et al. ¹⁰				Marchi et al. ¹¹ (for x_1 (R134a) higher than 0.7)			
T		BIASP	AADP	T		BIASP	AADP	T		BIASP	AADP
K	N	%	%	K	N	%	%	K	N	%	%
303.45	10	0.10	0.85	303.15	10	-5	7	303.24	20	-2	2
313.24	10	-0.23	0.98	313.15	10	-11	11	312.66	28	-0.9	0.9
323.33	14	-0.09	0.65	323.15	10	-14	14	322.82	28	-1	1
338.30	13	-0.21	0.79								
353.33	9	-0.65	1.01	353.15	10	-18	18				

^a N is the number of experimental measurements.

Table 9. PSRK Parameters, the van der Waals Properties, and the Interaction Parameters²⁶

group	subgroup	r_k	q_k	a_{ij}/K		
				40	1	13
40	CF ₃	1.4060	1.3800	0.00	147.30	278.15
	CF	0.6150	0.4600			
1	CH ₂	0.6744	0.5400	-2.859	0.00	251.5
13	CH ₂ O	0.9183	0.7800	-172.51	83.36	0.00
	CH ₃ O	1.1450	1.0880			

Table 10. Relative Deviations BIASP and AADP with Respect to the PSRK Model

R134a (1) + DMEDEG (2)			R134a (1) + DMETrEG (2)		
T	BIASP	AADP	T	BIASP	AADP
K	%	%	K	%	%
303.30	-14	14	303.45	-9	10
313.20	-8	9	313.24	-6	7
323.30	-7	7	323.33	-5	5
338.15	-5	6	338.30	-3	3
353.15	-4	4	353.33	-2	3

4.3. Comparison with the PSRK Model. The predictive Soave–Redlich–Kwong equation of state (PSRK EoS),²⁵ which is a combination of the Soave–Redlich–Kwong (SRK) equation of state with the universal quasichemical functional group activity coefficient (UNIFAC) model using PSRK mixing rules, is generally used to predict VLE data. The PSRK EoS with the Mathias–Copeman α function was chosen to predict the VLE data of the R134a + DMEDEG and R134a + DMETrEG binary systems. The Mathias–Copeman parameters were all taken from Table 4. The decomposition of the considered components in subgroups is presented with the subgroup parameters²⁶ in Table 9.

Because of the high values of the relative and systematic deviations (see the BIASP and AADP shown in Table 10), it is concluded that the PSRK EoS is not accurate enough to predict the phase equilibrium data for the R134a + DMEDEG and R134a + DMETrEG binary systems.

5. Conclusions

The isothermal solubility measurements were carried out using a “static–analytic” method, for R134a + DMEDEG and R134a + DMETrEG mixtures at temperatures from (303 to 353)

K and pressures up to 2.6 MPa with an uncertainty on the liquid mole fractions estimated to $\pm 3\%$. The experimental data were correlated by means of the PR-EoS with the Mathias–Copeman α function along with Huron–Vidal mixing rules and the NRTL activity coefficient model. Direct measurements and parameter adjustment using the PR-EoS¹⁸ with the Mathias–Copeman¹⁹ α function, Huron–Vidal²⁰ mixing rules, and the NRTL²¹ activity coefficient model allows accurate representation, with the AADP below 1%, while the PSRK EoS gives large deviations (AADP between 3 and 14%).

The PSRK model gives nonaccurate predicted data for both systems. Experimental data presented herein will be used in the near future to evaluate the performance of an AHT working with the R134a + DMEDEG and R134a + DMETrEG binary systems.

Literature Cited

- Zheng, D.; Ji, P.; Qi, J. Maximum excess Gibbs function of working pairs and absorption cycle performance. *Int. J. Refrig.* **2001**, *24*, 834–840.
- Shi, L. J. Y.; Zhu, M. S.; Han, L. Z. Performance analysis of an absorption heat transformer with different working fluid combinations. *Appl. Energy* **2000**, *67*, 281–292.
- Herold, K. E.; Radermacher, R.; Klein, S. A. *Absorption Chillers and Heat Pumps*; CRC Press: Boca Raton, FL, 1996.
- Zhuo, C. Z.; Machielsen, C. H. M. Performance of high-temperature absorption heat transformers using Alkilate as the working pair. *Appl. Therm. Eng.* **1996**, *16*, 255–262.
- Ishida, M.; Ji, J. Graphical exergy study on single stage absorption heat transformer. *Appl. Therm. Eng.* **1999**, *19*, 1191–1206.
- Shiming, X.; Yanli, L.; Lisong, Z. Performance research of self regenerated absorption heat transformer cycle using TFE-NMP as working fluids. *Int. J. Refrig.* **2001**, *24*, 510–518.
- Borde, I.; Jelinek, M.; Daltrophe, N. C. Working fluids for an absorption system based on R124 (2-Chloro-1,1,1,2-tetrafluoroethane) and organic absorbents. *Int. J. Refrig.* **1997**, *20*, 256–266.
- Fatouh, M.; Murthy, S. S. Comparison of R22-absorbent pairs for vapour absorption heat transformers based on P-T-X-H data. *Heat Recovery Syst. CHP* **1993**, *13*, 33–48.
- Borde, I.; Jelinek, M.; Daltrophe, N. C. Absorption system based on refrigerant R134a. *Int. J. Refrig.* **1995**, *18*, 387–394.
- Coronas, A.; Mainar, A. M.; Patil, K. R.; Conesa, A.; Shen, S.; Zhu, S. Solubility of 1,1,1,2-Tetrafluoroethane in Triethylene Glycol Dimethyl Ether. *J. Chem. Eng. Data* **2002**, *47*, 56–58.
- Marchi, P.; Scalabrin, G.; Ihmels, E. C.; Fischer, K.; Gmehling, J. Bubble pressure measurements for the (1,1,1,2-tetrafluoroethane + triethylene glycol dimethyl ether) system. *J. Chem. Thermodyn.* **2006**, *38*, 1247–1253.

- (12) López, E. R.; Mainar, A. M.; García, J.; Urieta, J. S.; Fernández, J. Experimental and Predicted Solubilities of HFC134a (1,1,1,2-Tetrafluoroethane) in Polyethers. *Ind. Eng. Chem. Res.* **2004**, *43*, 1523–1529.
- (13) Marchi, P.; Scalabrin, G.; Ihmels, E. C.; Fischer, K.; Gmehling, J. $P\rho T_x$ Measurements for (1,1,1,2-Tetrafluoroethane + Triethylene Glycol Dimethyl Ether) at High Haloalkane Content. *J. Chem. Eng. Data* **2006**, *51*, 992–996.
- (14) Comunas, M. J. P.; Fernández, J.; Baylaucq, A.; Canet, X.; Boned, C. $P\rho T_x$ Measurements for HFC-134a + triethylene glycol dimethyl ether system. *Fluid Phase Equilib.* **2002**, *199*, 185–195.
- (15) Monsalvo, M. A.; Baylaucq, A.; Quinones-Cisneros, S. E.; Boned, C. High-pressure viscosity behavior of x 1,1,1,2-Tetrafluoroethane (HFC-134a) + (1- x) triethylene glycol dimethylether (TriEGDME) mixtures: Measurements and modeling. *Fluid Phase Equilib.* **2006**, *247*, 70–79.
- (16) Laugier, S.; Richon, D. New Apparatus to Perform Fast Determinations of Mixture Vapor-Liquid Equilibria up to 10 MPa and 423 K. *Rev. Sci. Instrum.* **1986**, *57*, 469–472.
- (17) Zehioua, R.; Coquelet, C.; Meniai, A. H.; Richon, D. Isothermal Vapor-Liquid Equilibrium Data of 1,1,1,2-Tetrafluoroethane (R134a) + Dimethylformamide (DMF) Working Fluids for an Absorption Heat Transformer. *J. Chem. Eng. Data*, DOI: 10.021/je900440t.
- (18) Peng, D. Y.; Robinson, D. B. A New Two Constant Equation of State. *Ind. Eng. Chem. Fundam.* **1976**, *15*, 59–64.
- (19) Mathias, P. M.; Copeman, T. W. Extension of the Peng-Robinson equation of state to complex mixtures: evaluation of the various forms of the local composition concept. *Fluid Phase Equilib.* **1983**, *13*, 91–108.
- (20) Huron, M. J.; Vidal, J. New Mixing Rules in Simple Equations of State for Representing Vapour-Liquid Equilibria of Strongly non-ideal Mixtures. *Fluid Phase Equilib.* **1979**, *3*, 255–271.
- (21) Renon, H.; Prausnitz, J. M. Local Composition in Thermodynamic Excess Functions for Liquid Mixtures. *AIChE J.* **1968**, *14*, 135–144.
- (22) *Dortmund Data Bank (DDB)*, Version 97; DDBST Software and Separation Technology GmbH: Oldenburg, Germany, 1997.
- (23) Åberg, E. R.; Gustavsson, A. G. Design and evaluation of modified simplex methods. *Anal. Chim. Acta* **1982**, *144*, 39–53.
- (24) Poling, B. E.; Prausnitz, J. M.; O'Connell, J. P. *The Properties of Gases and Liquids*, 5th ed.; McGraw-Hill Book Company: New York, 2000.
- (25) Holderbaum, T.; Gmehling, J. PSRK: A Group Contribution Equation of State based on UNIFAC. *Fluid Phase Equilib.* **1991**, *70*, 251–265.
- (26) Raal, J. D.; Mühlbauer, A. L. *Phase Equilibria: Measurement and Computation*; Taylor & Francis: London, 1999.

Received for review November 23, 2009. Accepted January 12, 2010.

JE9009915